Available online at www.sciencedirect.com

SciVerse ScienceDirect

Ceramics International 39 (2013) 6415–6425

CERAMICS INTERNATIONAL

www.elsevier.com/locate/ceramint

Surfactant-free dispersion of silver nanoparticles into MWCNT-aqueous nanofluids prepared by one-step technique and their thermal characteristics

B. Munkhbayar[a], Md.Riyad Tanshen[a], Jinseong Jeoun[a], Hanshik Chung[b], Hyomin Jeong[b,*]

[a]*Department of Mechanical and Precision Engineering, Gyeongsang National University, 445 Inpyeong Dong, Tongyeong, Gyeongnam 650-160, Republic of Korea*

[b]*Department of Mechanical and Precision Engineering, Institute of Marine Industry, Gyeongsang National University, 445 Inpyeong Dong, Tongyeong, Gyeongnam 650-160, Republic of Korea*

Received 18 December 2012; received in revised form 11 January 2013; accepted 22 January 2013
Available online 31 January 2013

Abstract

This paper reports a significant enhancement in the thermal conductivity of silver-nanoparticle-based aqueous nanofluids with the addition of negligible amounts of multi-walled carbon nanotubes (MWCNTs). The present work was conducted using purified MWCNTs/water nanofluids prepared by a wet grinding method. Silver nanoparticles were dispersed into the MWCNT/water nanofluids via a one-step method using pulse power evaporation, which was observed to improve the dispersibility and thermal conductivity of the nanofluids. A particle sizing system (PSS) and transmission electron microscopy (TEM) were used to confirm the size of silver nanoparticles in base fluids. The PSS measurement results reveal that the size of the silver nanoparticles was approximately 100 nm, which is in good agreement with the results obtained from TEM and SEM. The maximum absorbance (2.506 abs at a wavelength of 264 nm) and highest thermal conductivity enhancement (14.5% at 40 °C) were achieved by a fluid containing '0.05 wt% MWCNTs–3 wt% Ag' composite.

Keywords: B. Composite; C. Thermal conductivity; Dispersibility; Carbon nanotube; Silver nanoparticle

1. Introduction

One of the most significant scientific challenges in industry, including the microelectronics, transportation and manufacturing industries is cooling. Technological developments such as microelectronic devices operating at high speeds, high-power engines, and bright optical devices are driving an increase in overall thermal loading, requiring advances in cooling. The conventional method used to increase heat dissipation is to increase the area available for exchanging heat using a better heat-conducting fluid. However, this approach involves an undesirable increase in the size of thermal management systems; therefore, there is an urgent need for new and novel coolants that exhibit improved performance. The innovative concept of 'nanofluids' – heat transfer fluids consisting of nanoparticle suspensions – has been proposed as a solution to these challenges [1].

Nanofluids are a type of new engineering material composed of solid nanoparticles measuring 1–100 nm suspended in base fluids. The term "nanofluid" was coined in 1995 by Choi of Argonne National Laboratory, USA [2] to describe the material conceived to surpass the performance of common heat transfer liquids. Nanofluids prepared by dispersing nanoparticles into conventional heat transfer fluids are considered to be next-generation heat transfer fluids, as they offer exciting new ways of enhancing heat transfer performance relative to that of pure liquids. Therefore, their possible areas of application are in advanced cooling systems

*Corresponding author. Tel.: +82 55 640 3184.
E-mail addresses: muugii_3685@yahoo.com (B. Munkhbayar), hmjeong@gnu.ac.kr (H. Jeong).

0272-8842/$ - see front matter © 2013 Elsevier Ltd and Techna Group S.r.l. All rights reserved.
http://dx.doi.org/10.1016/j.ceramint.2013.01.069

and micro/nano-electromechanical devices as well as in thermal management systems, viz. heat exchangers, industrial cooling applications and solar energy [3–5].

Over the past decade, researchers have used several types of solid nanoparticles such as (i) metallic particles [6,7] (Cu, Al, Fe, Au, and Ag), (ii) nonmetallic particles [8,9] (Al_2O_3, CuO, Fe_3O_4, TiO_2, and SiC) and (iii) carbon nanotubes [10,11] as additives in nanofluids. Among the metallic and nonmetallic particles, Ag nanoparticles [12,13] have gained significant attention owing to their potential applications as well as low cost and high thermal conductivity. The key step in improving the thermal conductivity of fluids using nanoparticles is synthesis. There are two main techniques used to synthesize nanofluids: (i) the one-step direct evaporation method, through which nanoparticles are directly formed within base fluids, and (ii) the two-step method, through which nanoparticles are formed and subsequently dispersed in base fluids. Compared to the two-step method, the one-step process has many advantages, such as smaller particle size, less contamination of the particle surface, and high dispersion stability. However, the one-step process only produces nanofluids in small quantities, and the produced nanofluids are expensive. Furthermore, the volume concentration of nanoparticles is much more limited in the one-step process compared with that in the two-step technique. To resolve this issue, the pulsed-wire evaporation (PWE) method [14–16] was used to synthesize nanofluids in the present work. In particular, the product mass of nanoparticles can be controlled by changing the wire explosion number [16].

Because of their very high thermal conductivity (3000–6000 W/m K) and very large aspect ratio [17,18], CNTs are expected to be promising in preparing nanofluids with enhanced thermal conductivity. Moreover, CNTs have attracted great interest from researchers because of their unique structure and resultant electrical, optical and mechanical properties [19,20]. However, there are two main issues facing their application in structural materials. First, the entanglement of CNTs occurs due to their long and winding shapes, as well as the van der Waals forces between them. Second, weak interfacial interactions occur between CNTs and their surrounding matrix due to the hydrophobic surfaces of CNTs. In our previous work [21,22], these issues were successfully resolved by incorporating acid oxidation, ultrasonication and planetary ball milling processes under wet conditions. It was found that both the dispersibility and thermal conductivity of MWCNT nanofluids could be significantly enhanced using a grinding method assisted by dispersion at high rotational speeds. Moreover, our previous studies show that highly stable MWCNT nanofluids can be synthesized.

In addition, using a surfactant is an effective way to improve the dispersibility of nanoparticles in base fluids [23,24]. The surfactant approach changes the wetting or adhesion behavior of the nanoparticles, which helps reduce their tendency to agglomerate. Rastogi et al. [24] compared the dispersion of MWCNTs treated with four surfactants: Triton X-100, Tween 20, Tween 80, and sodium dodecyl sulfate (SDS). It has been suggested that the proper choice of a suitable surfactant requires consideration of its structure, optimum volume fraction relative to that of nanotubes, and solution stability. However, in nanofluid applications, although surfactants can improve the dispersion stability, it may cause several problems such as contamination of the heat transfer media and the production of foams. Furthermore, surfactant molecules adsorbed on the surface of CNTs may enlarge the thermal resistance between the CNTs and the base fluid, which limits the enhancement in the effective thermal conductivity [25]. Thus, no surfactants were used in the present work.

The addition of negligible amounts of CNTs to metallic and metallic oxide nanofluids opens new ways of obtaining versatile performance characteristics. To date, a much attention has been given to the decoration of CNTs with nanoparticles composed of metals [26–28], metal oxides [29,30], or metal sulfides [31,32] due to the composites' special catalytic [33], electrical, magnetic, thermal, and optical properties [34,35]. However, very few reports are available on the synthesis of nanofluids with Ag nanoparticles (Ag-NPs) attached to CNTs (Ag/CNTs) [36,37], which exhibit excellent chemical and physical stability.

In this manuscript, a one-step method was applied to synthesize the Ag/MWCNTs composite nanofluids with different 'Ag-NPs' loadings (1 wt%, 2 wt% and 3 wt%). The dispersibility and thermal conductivity of these nanofluids were measured and analysed. The objective of this study was three-fold: (i) to improve the dispersibility and thermal conductivity of MWCNT nanofluids by incorporating acid oxidation, ultrasonication and planetary ball milling processes under wet conditions; (ii) to synthesize 'Ag' nanofluids using a simple one-step process via the PWE technique involving the simultaneous preparation and direct dispersion of nanoparticles in base fluids; and (iii) to enhance the thermal conductivity of metallic 'Ag' nanofluids by preparing Ag/MWCNT composite nanofluids with negligible amounts of added MWCNTs. Based on the experimental results, we discuss the reasons for the enhancement and/or decrement in the dispersion and thermal characteristics of the nanofluids.

2. Experiment

2.1. Materials

MWCNTs measuring ~20 nm in diameter and ~5 μm in length and with greater than 95% purity, less than 3% impurities and a specific surface area of 40–300 m^2/g (purchased from Carbon Nanomaterial Technology Co., Ltd, South Korea) were synthesized by chemical vapour deposition (CVD). Pure 'Ag' (>99.9%) wire with a diameter of 0.2 mm (purchased from Nano Technology Inc. Korea) was used as the starting material. Distilled water (DI water) was used as the base fluid of the nanofluids.

2.2. Preparation of MWCNTs nanofluids

One of the critical steps in preparing carbon nanofluids is dispersing CNTs in a base fluid. Due to the high aspect ratio and strong Van der Waals forces between carbon surfaces, the dispersion of CNTs in aqueous media can be challenging. CNTs are hydrophobic in nature and thus cannot be dispersed in water under normal conditions [5,21]. MWCNTs were polarized by chemical treatment to allow for better dispersion. A simple method for purifying MWCNTs by using nitric acid (HNO_3) and sulfuric acid (H_2SO_4) was employed [22,30]. The MWCNTs were purified by performing ultrasonication in Branson ultrasonic cleaner model 1510E –DTH (Branson Ultrasonic Corporation 41, Danbury, CT 06813, USA) for 5 h to remove impurities and amorphous carbon and to improve the nanotubes' exterior activity. Calorimetry was performed to measure the output power and frequency of the applied ultrasonic vibration: 63 W and 42 KHz, respectively. The details of purification process have been previously described [5,21,22,and30]. The resulting sample yielded 0.7 g of purified MWCNTs, which was used for the next step in the experiment, as described below. The structure, size and purity of the raw and purified CNTs were confirmed by transmission electron microscopy (TEM) (JEM-2100 F, JEOL; Tokyo, Japan). In addition, the dispersion states were imaged by digital photography to evaluate the purification process in terms of the dispersibility of the MWCNTs.

One of the reasons that MWCNTs cannot be completely dispersed in base fluids is their long length. A planetary ball mill (HPM-700) (Haji Engineering, Korea) was used to enhance the dispersibility of the MWCNT nanofluids by shortening the length of the nanotubes. Monosized (3.0 mm) spherical zirconia (ZrO_2) balls (Haji Engineering, Korea) were used as the collision medium. The grinding process has been described in our previously published article [5]. The agitator-applied rotation speed was 500 rpm, and the grinding time of the MWCNTs under wet conditions was 1 h. The extent to which the nanotubes were shortened was analyzed by scanning electron microscopy (SEM) (JSM-5610, JEOL, and Tokyo, Japan).

For better dispersion, the purified and ground MWCNTs were ultrasonically dispersed in an aqueous solution for 40 min. Ice water was repeatedly added to the ultrasonic bath during ultrasonication to prevent an increase in the temperature of the suspension. The stabilities of the nanofluids were examined approximately 40 h after ultrasonication. The concentration of MWCNTs in aqueous solution was adjusted to 0.05 wt%. To compare the dispersibility and thermal conductivity of the raw and treated MWCNTs nanofluids, a UV spectrophotometer (X-ma 3000 Series Spectrophotometer, Human Co., Ltd, Korea) operating at wavelengths ranging from 200 to 800 nm and a thermal conductivity analyser (LAMBDA, F5 Technologie GmbH, Willingshausen, Germany) operating at temperatures of 15–40 °C in intervals of 2.5 °C were used in the present work. The LAMBDA system measures the thermal conductivity of fluids according to ASTM D 2717. The operation of the instrument was based on the working principles of the transient hot wire method used for nanofluids [21,38]. The sample temperature was controlled by a special double-jacket heating/cooling device, which provides a homogeneous temperature distribution. Moreover, the UV–visible spectrometry measurements were used to qualitatively characterize the colloidal stability of the dispersions.

2.3. 'Ag' and 'Ag/MWCNTs' nanofluids preparation

'Ag'- and 'Ag/MWCNTs'-nanoparticle-based aqueous nanofluids were prepared by a one-step physical technique using the PWE method (Portable, Nano Colloid Maker, Nano Technology Inc., Korea). The apparatus used consists of four main components: a high-voltage DC power supply, a capacitor bank, a high-voltage gap switch, and an evaporation/condensation chamber. The feeding length of the wire into the reaction chamber was 90 mm. When a high-voltage pulse of 300 V is driven through a thin wire, the non-equilibrium overheating induced in the wire causes the wire to evaporate into plasma within several microseconds. The high-temperature plasma is cooled by interaction with an argon-oxygen mixed gas and condensed into small particles.

First, a DI-water-based 'Ag' nanofluid with a nanoparticle concentration of 2 wt% was prepared by the one-step PWE method to examine the morphology and size of the synthesized 'Ag' nanoparticles. The morphology and size of the 'Ag' nanoparticles were examined by SEM and TEM. To measure the 'Ag' particle size, a particle sizing system (PSS, NICOMP 380, and Santa Barbara, California, USA) was used in the present study.

'Ag/MWCNT' composite nanofluids were prepared using the following procedure. The previously prepared 0.05 wt% MWCNTs nanofluids were poured into a 500 ml exploding bottle, which was then installed in the main part of the PWE instrument. Then, 'Ag' nanoparticles were synthesised by the PWE method and made direct contact with the base fluid inside the chamber wall. A DI-water-based nanofluid containing 'Ag/MWCNTs' nanoparticles without any surface contamination was finally obtained. The 'Ag/MWCNTs' nanofluids were prepared with a constant concentration of MWCNTs (0.05 wt%) and three different concentrations of 'Ag' nanoparticles (1 wt%, 2 wt% and 3 wt%). The concentration of 'Ag' nanoparticles in aqueous solution and/or in the MWCNT-aqueous nanofluids was controlled by adjusting the wire explosion number. The structural and morphological properties of these 'Ag/MWCNTs' nanofluids were studied by TEM. The dispersibility and thermal conductivity of these nanofluids were measured by UV spectrophotometry and a transient short hot wire method [38].

3. Results and discussion

3.1. Characterization of the MWCNT nanofluids

It should be noted that raw CNTs generally floated and were difficult to disperse in base fluids (distilled water, anhydrous ethanol, etc.), which could be due to the large aspect ratio and the lack of surface functional groups, despite the fact that the density of the MWCNTs (1.8 g cm^{-3}) is slightly larger than that of water and anhydrous ethanol. A simple method for purifying the MWCNTs using nitric and sulfuric acid was employed in this work. In the purification process, the catalyst on the tube surface was removed, and the tube caps were opened, as confirmed by Fourier-transform infrared (FTIR) spectra reported in the literature [39]. After purification, similar MWCNT characteristics were observed in the TEM images. Fig. 1 shows high-magnification TEM images of raw and purified MWCNTs. The images show that the raw MWCNTs contain large amounts of impurities, such as catalyst particles, amorphous carbon, carbon particles and multi-shell carbon nanocapsules (red arrows in Fig. 1a). The catalyst particles are evidently embedded in the tips or the tube cores of the MWCNTs. The outer walls of the raw MWCNTs were coated with a layer of amorphous carbon, which can be clearly observed in Fig. 1a. In contrast, the purified MWCNTs were clean and possessed no carbon particles, as shown in Fig. 1b. Interestingly, the structures of the amorphous carbon and carbon particles of the raw MWCNTs were completely eliminated, and the tips of the nanotubes opened (yellow arrows, Fig. 1b) after purification. The amount of amorphous carbon was relatively small, graphite was virtually absent, and the catalyst metal particles could be eliminated by a relatively brief treatment with acid. The same morphology and tubular structure of the MWCNTs were observed, as shown in Fig. 1b, suggesting that the structural integrity of the CNTs was not deteriorated and that the crystal structure of the MWCNTs remained unchanged after purification.

It is well established that the purification of MWCNT removes impurities and agglomerations of raw materials; consequently, the pure structure allows MWCNTs to disperse well in base fluids. Fig. 2 shows the dispersion states of raw and purified MWCNTs in aqueous solution. Fig. 2a shows the dispersion state of raw MWCNTs particles in aqueous solution, demonstrating that large amounts of particles aggregated on the surface of the water and along the wall of the bottle instead of being dispersed, despite the application of ultrasonication. This aggregation of raw MWCNTs is known to be due to a lack of hydrophilic groups in their structure, prohibiting interaction with the polar solvent, as described above. By contrast, Fig. 2b shows that the nanofluid containing purified MWCNTs exhibits better dispersion. The rest of the purified MWCNTs remained as colloidal (well-dispersed) solutions for several days, without an appreciable change in their dispersion state after ultrasonication. As indicated by optical inspection, it is clear that the presence of functional groups in the oxidized MWCNTs led to a reduction in the van der Waals interactions between them, which promoted their separation and dispersion in water.

However, it was found in a recently published work [5,21] that the presence of hydrophilic groups is generally insufficient in allowing complete dispersion due to the large hydrophobic surface area of CNTs. This phenomenon might be associated with the attractive forces induced by the large hydrophobic specific surface and long length of the CNTs, even after acid treatment [40]. Thus, to further improve the dispersibility of the MWCNT nanofluids, planetary ball milling was applied [21,22] at a rotational speed of 500 rpm. To determine how well the purification and grinding assisted in the dispersion of the MWCNT nanofluids, the samples were analyzed by UV spectrophotometry. In addition, the dispersibility of nanoparticles in the base fluid can be characterized using UV–vis absorption spectroscopy. Generally, higher absorbance indicates better dispersion and solubility of the nanoparticles in solution. To characterize the dispersion of the MWCNT suspensions using UV–vis spectroscopy, absorbance values were recorded at a wavelength of approximately 260 nm, as reported Yu et al. [41]. The Lambert–Beer law is well obeyed by CNTs at this wavelength. Fig. 3 shows that the

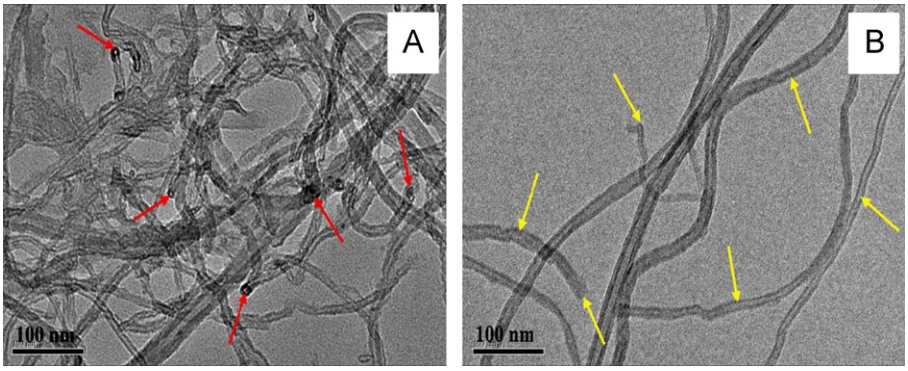

Fig. 1. High-magnification TEM images of (a) raw and (b) purified MWCNTs. (For interpretation of the references to colour in this figure caption, the reader is referred to the web version of this article.)

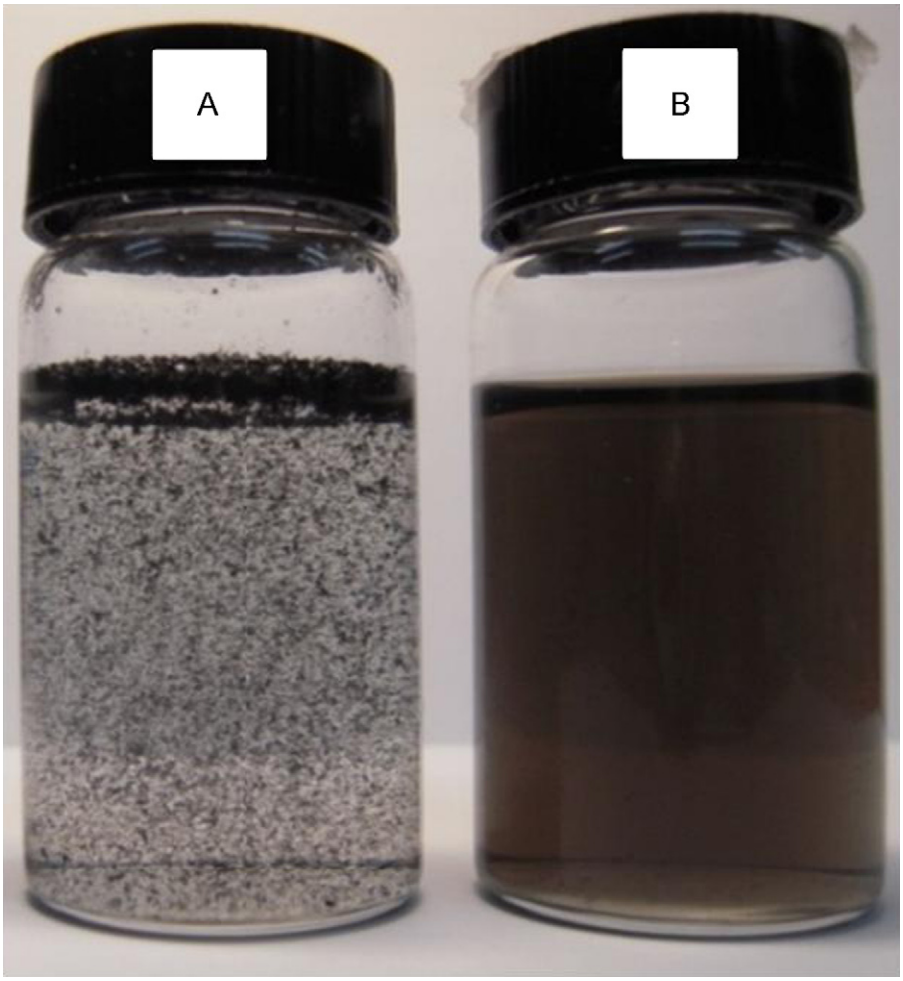

Fig. 2. Photograph of the (a) raw and (b) purified MWCNTs in aqueous solution.

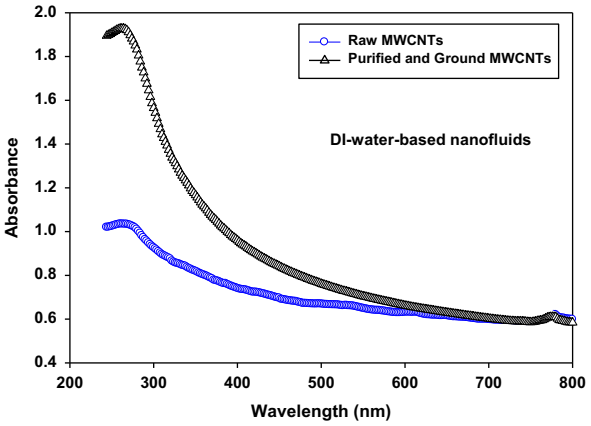

Fig. 3. UV light absorption measurements of the raw and purified and ground MWCNTs structures in an aqueous solution.

highest absorbance peak of the MWCNTs in aqueous solution was recorded at a wavelength of 264 nm. Fig. 3 shows the UV–vis spectra of the raw and purified and ground MWCNTs nanofluids. As shown, the lowest absorbance (1.034 abs) was measured for the raw MWCNT suspension, despite the application of ultrasonication. This poor dispersion of raw MWCNTs in aqueous solution is due to the large degree of particle aggregation, as described above. Meanwhile, the purified and ground MWCNT suspension exhibited much higher absorbance (1.928 abs) than the raw MWCNT nanofluid, despite the fact that the samples were prepared in the same concentration. This significant improvement in dispersibility can be attributed to several factors: (i) the purified structure of the MWCNTs allows for better dispersion in the base fluid; (ii) grinding was effective in shortening the length of the nanotubes, and thereby, the shortened MWCNTs were well dispersed in the base fluid [5,42]; and (iii) grinding was able to break up large MWCNT aggregates into smaller ones, and furthermore, exfoliation could be employed to break these smaller aggregates into individual nanotubes, which would facilitate ultrasonication in dispersing the MWCNTs, as described in our previously published work [42]. It is well known that individual CNTs are highly active in the UV–vis region and exhibit characteristic bands corresponding to additional absorption due to Van Hove singularities [41]. CNTs bundles, however, are hardly active in the wavelength region of 200–1000 nm, where their photoluminescence is quenched [24].

Fig. 4 confirms the breaking of large particles into individual nanotubes and the shortening of MWCNTs described above. Fig. 4 shows SEM images of raw and

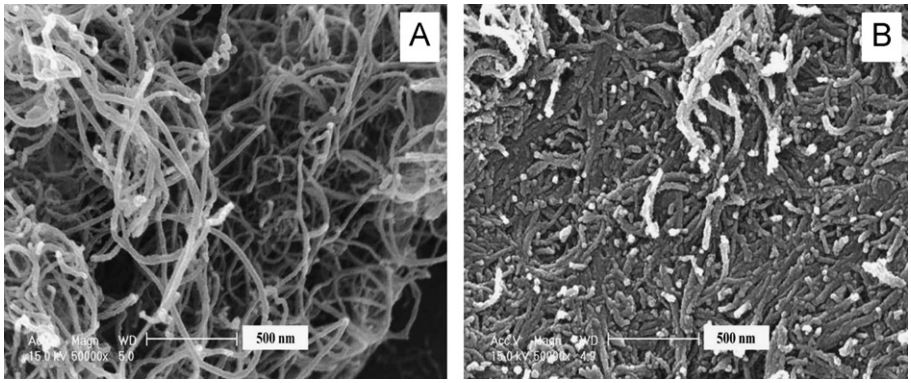

Fig. 4. SEM images of the (a) raw and (b) ground MWCNT structures.

ground MWCNTs under wet conditions at a rotational speed of 500 rpm. The images reveal that the length of nanotubes decreased following high-energy milling. As shown in Fig. 4a, the length of the raw MWCNTs is far longer than 500 nm. Furthermore, Fig. 4b shows that grinding at a rotational speed of 500 rpm lead to particle breakage. During the grinding process, the powder mixtures were subjected to high-energy inter-particle and milling-ball collisions at high rotational speeds. Thus, particle breakage occurred due to the relative impact velocity of balls colliding with each other or against the mill, pot and wall during grinding. As shown in Fig. 4b, the length of the ground MWCNTs was clearly shorter than 500 nm, which corroborates the aforementioned explanation.

In this study, one of the objectives was to enhance the thermal conductivity of fluids containing MWCNTs. The thermal conductivity of the fluid containing MWCNTs was measured to further examine the effects of the grinding process. The effective thermal conductivity (K_{eff}, ratio of thermal conductivity of nanofluids (K_{nf}) to that of base fluid (K_{bf})) of the MWCNT nanofluids with respect to temperature is presented. The effective thermal conductivity is greatly affected by the interfacial contact resistance between surfaces and samples, as well as that between sample particles [43]. Fig. 5 presents the effective thermal conductivities of fluids containing raw and purified and ground MWCNTs measured at temperatures ranging from 15 °C to 40 °C. It is clear that the thermal conductivity of the fluid containing both MWCNT structures increased linearly with temperature. This enhancement in thermal conductivity as a function of temperature is due to an enhanced Brownian motion effect [44]. A detailed explanation of this enhancement will be described below. Meanwhile, as shown in Fig. 5, the effective thermal conductivity of the fluid containing purified and ground MWCNTs was higher than that of the raw MWCNT nanofluids.

In our previously published articles [21,22], the possible reasons for the increment in the thermal conductivity of MWCNTs nanofluids due to grinding are the following: (i) the straightness ratio, (ii) specific surface area and

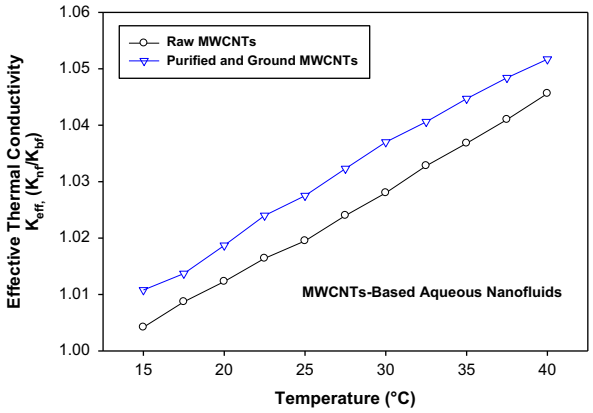

Fig. 5. Effective thermal conductivity of the raw and treated CNT nanofluids vs. temperature.

(iii) the significant role played by aggregation in heat transfer. (i) It is known that the walls of CNTs have a similar structure to that of graphene sheets and the thermal conductivity of CNTs shows greatly anisotropic behavior. Heat is transported substantially more rapidly along the axial direction than along the radial direction [45]. Xie and Chen [46] reported that the straightness ratio is significantly increased and heat is transported more effectively through CNTs and across the interfaces between CNT tips and base fluids, resulting in a large thermal conductivity enhancement in nanofluids containing CNTs. A more detailed mechanism of this thermal conductivity enhancement in a nanofluid due to the straightness ratio is described in the literature [46]. The SEM images of ground MWCNTs shown in Fig. 4 confirm the proposed increase in the straightness ratio. (ii) Xuan and Li [47] listed the reasons for the significant improvement in the heat transfer performance of nanofluids. Among the reasons, the increase in the specific surface area of suspended nanoparticles and the interaction and collision between particles can explain the increased thermal conductivity of nanofluids due to grinding. It should be noted that grinding is effective in increasing the specific surface area and thereby significantly reduces the agglomeration of MWCNTs [48]. In this study, an improvement in the specific surface area

by grinding was clearly observed, as shown in Fig. 4. Therefore, when the specific surface area increases, the interaction and collision between particles is enhanced. (iii) Decreasing the aggregation of MWCNTs may affect an improvement in thermal conductivity [49]. In this study, the aggregation of MWCNT nanofluids was successfully reduced by grinding, which resulted in the high dispersion stability of the nanofluids. Moreover, it was found that the grinding process separated aggregates into individual CNTs. It is well understood that nanofluids with individual CNTs transport heat more rapidly than those with aggregated and/or bundled particles.

3.2. Characterization of the 'Ag' and 'Ag/MWCNTs' nanofluids

'Ag' nanoparticles were synthesized and dispersed in MWCNT nanofluids by a one-step PWE method. Before characterizing the 'Ag/MWCNT' composite nanofluids, the structural and morphological properties and size of the 'Ag' nanoparticles by synthesized by the PWE method were studied. The inset of Fig. 6 shows the dispersion state of 'Ag' nanoparticles in aqueous solution at a concentration of 2 wt%. As shown, the 'Ag' nanoparticles in the base fluid were well dispersed and no sedimentation was observed, even after several days. The colour of the solution is typical of a silver nanofluid. An SEM image of 'Ag' nanoparticles is shown in Fig. 6a; the figure shows the distribution and shape of the particles, which are nearly spherical. Moreover, 'Ag' nanoparticles measuring approximately 100 nm in size and exhibiting very smooth surfaces can be observed. Fig. 6b shows a typical TEM image of 'Ag' nanoparticles of different sizes prepared by the PWE method. As shown, the 'Ag' nanoparticles are spherical in shape and smaller than 100 nm.

To confirm the 'Ag' particle size, the synthesized 'Ag' nanofluid sample was examined by a particle sizing system. As shown in Fig. 7, the mean size of the silver nanoparticles determined by PSS varies from 60 to 150 nm. Moreover, it can be seen that the highest intensity peak occurs in the range of approximately 80–90 nm, which is in good agreement with the particle size measured using the SEM and TEM images. However, it can be observed that a very small intensity peak occurs in the particle size range between 120 and 150 nm, which may be attributed to particle agglomeration in the base fluid. Overall, the one-step method was found to be effective in producing nanosized particles in the base fluid.

The main objective of this study was to improve the dispersibility and thermal conductivity of 'Ag'-nanoparticle-based aqueous nanofluids by adding negligible amounts of MWCNTs. Fig. 8 compares the UV–vis spectra of the 'Ag/MWCNTs' composite nanofluids with different 'Ag-NPs' loadings (1 wt%, 2 wt% and 3 wt%) prepared by the PWE method with those of a fluid containing only MWCNTs. The fluid containing MWCNTs presents very high absorbance (1.928) at a wavelength of 264 nm, which demonstrates the high dispersibility of the MWCNT nanofluids. It is known that the MWCNTs in the base fluid are strongly active over the wavelength range of 240–400 nm [24,41,49]. However, CNTs are hardly active at wavelengths above 400 nm. Compared to those of the fluid containing only MWCNTs, the UV spectra of the 'Ag/MWCNT' nanofluids show higher absorbance over the wavelength range of 400–800, which is due to the addition of 'Ag' nanoparticles. It should be noted that silver nanoparticles generally shows high UV absorbance at wavelengths ranging between 400 and 800 nm [50]. Thus, the composition of the 'Ag/MWCNT' composites is vital in tailoring the composites to various applications. Among the 'Ag/MWCNT' composites, the absorbance peak height of the 'MWCNT–1 wt% Ag' nanofluid is the smallest, that of the 'MWCNT–2 Ag'wt% nanofluid is intermediate and that of the 'MWCNT–3 wt% Ag' nanofluid is the highest. This trend is due to the concentration of silver nanoparticles in the base fluid. Therefore, the absorbance peaks of the composite nanofluids were higher than the absorbance peak of the fluid containing only MWCNTs, which means that the

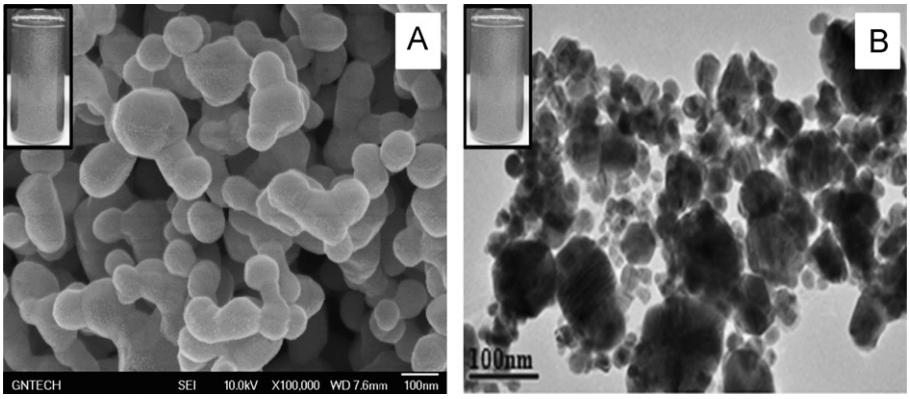

Fig. 6. High-magnification (a) SEM and (b) TEM image of the 'Ag' nanoparticles synthesised by the PWE method. The inset shows a digital photograph of 'Ag' nanoparticles dispersed in aqueous solution.

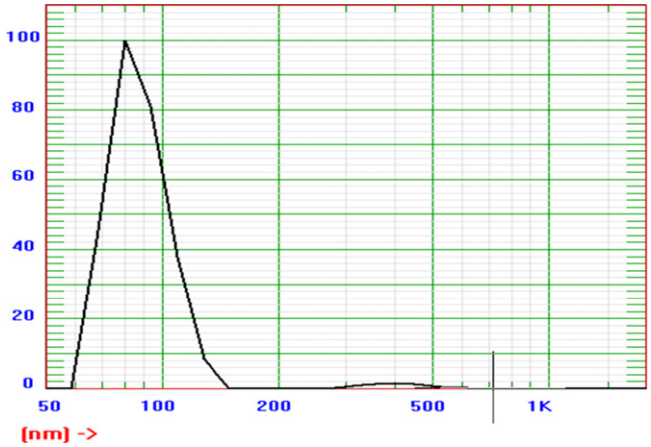

Fig. 7. Particle size vs. intensity of 'Ag' nanoparticles in aqueous solution prepared by one-step PWE method.

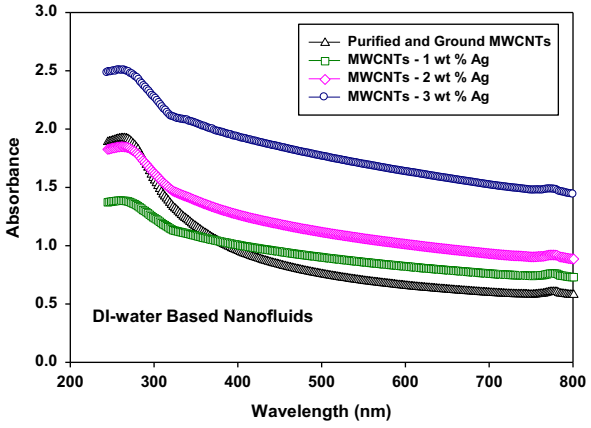

Fig. 8. UV light absorption measurements of the 'Ag/MWCNT' composite nanofluids with different 'Ag-NP' loadings prepared by PWE method compared those for a fluid containing only CNTs.

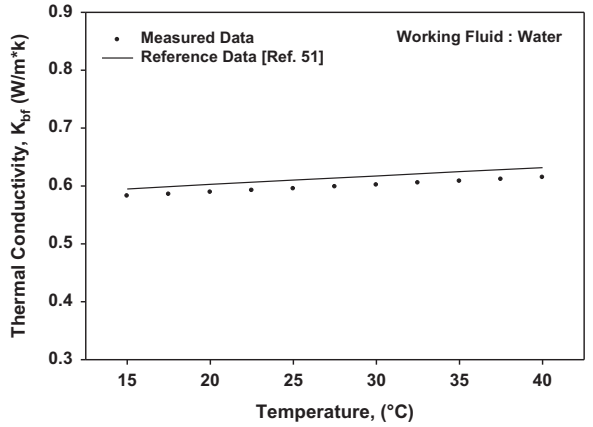

Fig. 9. Comparison of the measured thermal conductivity data for the base fluid (distilled water) with reference data [51].

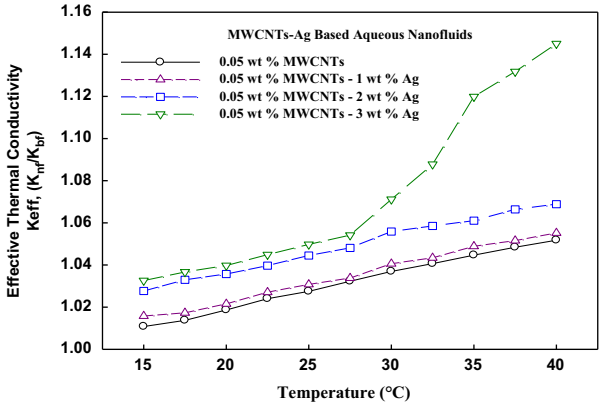

Fig. 10. Effective thermal conductivity of the 'Ag/MWCNT' composite nanofluids with varying 'Ag-NP' loadings prepared by PWE method and compared with a fluid containing only CNTs.

degree of dispersion of the composite nanofluids might be higher than that of the nanofluids containing only CNTs.

It is of great interest to be able to prepare a stable nanofluid with high thermal conductivity. The thermal conductivity of nanofluids is a transport property that is important to their practical application. Before measuring the thermal conductivity of the nanofluids, the Lambda system was calibrated using the base fluid (distilled water). Then, the measured data were compared with the reference data presented in a standard textbook [51]. As shown in Fig. 9, the measured and reference values are in relatively good agreement and the uncertainty in the thermal conductivity measurement is approximately 2.0%.

Because silver exhibits high thermal conductivity, the decoration of MWCNTs with 'Ag' may also increase the thermal conductivity of composite nanofluids. The temperature dependence of the effective thermal conductivities of composites with varying 'Ag-NPs' contents is illustrated in Fig. 10; these data are compared with those obtained for the fluid containing only MWCNTs. The thermal conductivity of the nanofluids was observed to increase linearly with temperature. One of the suggested reasons behind this phenomenon is an enhanced Brownian motion effect. Jang and Choi [44] suggested that as the temperature increases, the viscosity of the nanofluid decreases, which results in an increase in the Brownian motion of nanoparticles. It has been postulated that convection-like effects are induced by Brownian motion, which result in increased apparent thermal conductivities. On the other hand, it can be observed that the thermal conductivity of the composite nanofluids increases with 'Ag-NP' loading at any temperature.

Moreover, it can be seen that the 'Ag/MWCNT' composite nanofluids show a higher thermal conductivity than that of the fluid containing only MWCNTs. The higher thermal conductivity is attributed to the improved dispersion of CNTs in the matrix, as well as the decoration of the MWCNTs with silver, which enhanced the contact conductance of the CNTs throughout the network they formed in the matrix. Because silver itself is a good thermal conductor (K_{Ag}=429 W/m K), the 'Ag/MWCNT' interface facilitates phonon conduction by reducing boundary

Table 1
Thermal conductivity enhancement of the 'Ag/MWCNTs' suspensions varying 'Ag-NPs' loading prepared by one-step PWE method at a temperature of 40 °C.

Sample	Thermal conductivity enhancement (%), $((K_{nf}-K_{bf})/K_{bf}*100)$
0.05 wt% 'MWCNTs'	5.17
0.05 wt% 'MWCNTs'–1 wt% 'Ag'	5.52
0.05 wt% 'MWCNTs'–2 wt% 'Ag'	6.88
0.05 wt% 'MWCNTs'–3 wt% 'Ag'	14.5

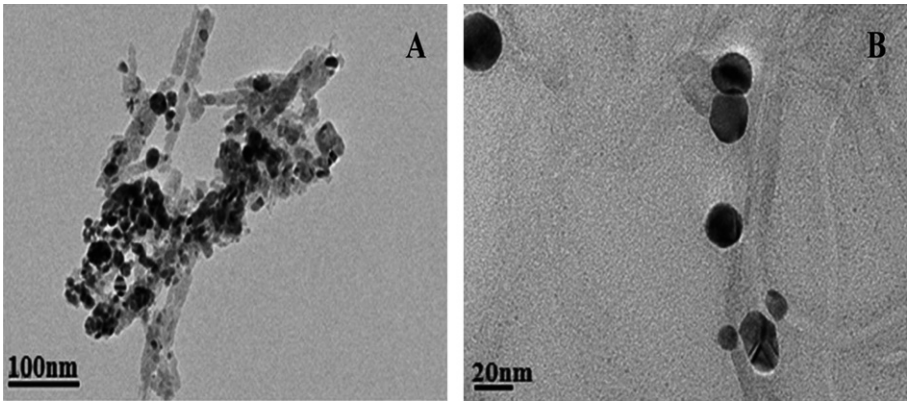

Fig. 11. (a) Low- and (b) high-magnification TEM image of 'Ag/MWCNT' composite structure.

scattering losses [52] and interfacial resistance to heat flow [53] between the 'Ag/MWCNT' interface and the polymer matrix. Therefore, the decoration of CNTs with 'Ag-NPs' offers an excellent means for recovering the potential reduction in thermal conductivity arising from the functionalization of CNTs. Data regarding the measured thermal conductivities of the nanofluids are shown in Table 1. The decoration of MWCNTs with silver can be confirmed by the TEM images of the 'Ag/MWCNT' composites.

Fig. 11 shows low- and high-magnification TEM images of an 'Ag/MWCNT' composite structure, which confirms the decoration of the MWCNTs with silver. As shown in Fig. 11a, several different-sized 'Ag' nanoparticles were attached to the MWCNTs. Fig. 11b clearly shows that silver nanoparticles were strongly adsorbed onto the MWCNT surfaces. Finally, a simple method was established for decorating CNTs with 'Ag' nanoparticles after purification and wet grinding.

4. Conclusion

The present study describes a significant enhancement in the thermal conductivity of silver-nanoparticle-based aqueous nanofluids by the addition of negligible amounts of MWCNTs. The dispersibility and thermal conductivity of the 'Ag/MWCNT' composite nanofluids was successfully enhanced using a one-step PWE method. It was demonstrated that grinding can significantly enhance the dispersion stability and thermal conductivity of MWCNT nanofluids. The enhanced dispersibility and thermal conductivity of the MWCNT nanofluids can be explained by (i) an increment in the straightness ratio increment, (ii) an improvement in the specific surface area and (iii) a reduction in aggregation. The one-step method was observed to be effective in producing nanosized particles in a base fluid. SEM, TEM and PSS measurements indicate that the size of the 'Ag-NPs' in aqueous solution was approximately 100 nm. The maximum absorbance (2.506 abs at a wavelength of 264 nm) and highest thermal conductivity enhancement (14.5% at 40 °C) were achieved in the fluid containing a '0.05 wt% MWCNT–3 wt% Ag' composite. This thermal conductivity enhancement was higher than that of the fluid containing only MWCNTs and is attributed to the improved dispersion of CNTs in the matrix, as well as silver decoration, which enhanced the contact conductance of the CNTs throughout the networks they formed in the matrix.

Acknowledgement

This research was supported by the Basic Science Program through the National Research Foundation of Korea (NRF) funded by the Ministry of Education, Science and Technology (No.2012-0004544).

Reference

[1] P. Keblinski, J.A. Eastman, D.G. Cahill, Nanofluids for thermal transport, Materials Today 8 (2005) 36–44.

[2] S.U.S. Choi, Enhancing thermal conductivity of fluids with nanoparticles, in: D.A. Siginer, H.P. Wang (Eds.), Developments and Applications of Non-Newtonian Flows, The American Society of Mechanical Engineers, New York, 1995, pp. 99–105 (FED-vol. 231/MD-vol. 66).
[3] B. Munkhbayar., J. Nine, J. Jeoun, M. Ji, H. Chung, H. Jeong, Synthesis of a graphene-tungsten composite with improved dispersibility of graphene in an ethanol solution and its use a counter electrode for dye-sensitized solar cells, Journal of Power Sources 230 (2013) 207–217.
[4] S.D. Seo, D.H. Lee, J.C. Kim, G.H. Lee, D.W. Kim, Room-temperature synthesis of CuO/graphene nanocomposite electrodes for high lithium storage capacity, Ceramics International 39 (2013) 1749–1755.
[5] B. Munkhbayar, Seunghwa Hwang, Junhyo Kim, Kangyoul Bae, Myoungkuk Ji, Hanshik Chung, Hyomin Jeong, Photovoltaic performances of dye-sensitized solar cells with various MWCNT counter electrode structures produced by different coating methods, Electrochimica Acta 80 (2012) 100–107.
[6] M.S. Liu, C.C. Lin, C.Y. Tsai, C.C. Wang, Enhancement of thermal conductivity with Cu for nanofluids using chemical reduction method, International Journal of Heat and Mass Transfer 49 (2006) 3028–3033.
[7] K. Gupta, P.C. Jana, A.K. Meikap, Optical and electrical transport properties of polyaniline–silver nanocomposite, Synthetic Metals 160 (2010) 1566–1573.
[8] Hafizur Rehman, B. Munkhbayar, H.M. Jeong, H.S. Chung, Sedimentation study and dispersion behavior of Al_2O_3–H_2O nanofluids with dependence of time, Advanced Science Letters 6 (2012) 96–100.
[9] D. Chen, H. Liu, S. Xia, One-step decomposition of basic carbonates into single-phase crystalline metallic oxides nanoparticle by ultrasonic wave-assisted ball milling technology, Ceramics International 38 (2012) 821–825.
[10] A.M.Jacobi Binglu Ruan, Heat transfer characteristics of multiwall carbon nanotube suspensions (MWCNT nanofluids) in intertube falling-film flow, International Journal of Heat and Mass Transfer 55 (2012) 3186–3195.
[11] P. Hvizdoš, V. Puchý, A. Duszová, J. Dusza, C. Balázsi, Tribological and electrical properties of ceramic matrix composites with carbon nanotubes, Ceramics International 38 (2012) 5669–5676.
[12] H. Lotfi, M.B. Shafii, Boiling heat transfer on a high temperature silver sphere in nanofluid, International Journal of Thermal Sciences 48 (2009) 2215–2220.
[13] M. Haji, T. Ebadzadeh, M.H. Amin, M. Kazemzad, T. Talebi, Gelcasting of Al2O3/Ag nanocomposite using water-soluble solid-salt precursor, Ceramics International 38 (2012) 867–870.
[14] Y.R. Uhm, J.H. Park, W.W. Kim, C.H. Cho, C.K. Rhee, Magnetic properties of nano-size Ni synthesized by the pulsed wire evaporation (PWE) method, Materials Science and Engineering B 106 (2004) 224–227.
[15] H.M. Lee, Y.R. Uhm, C.K. Rhee, Phase control and characterization of Fe and Fe-oxide nanocrystals synthesized by pulsed wire evaporation method, Journal of Alloys and Compounds 461 (2008) 604–607.
[16] G.J. Lee, C.K. Kim, M.K. Lee, C.K. Rhee, S. Kim, C.Y. Kim, Thermal conductivity enhancement of ZnO nanofluid using one-step physical method, Thermochimica Acta. 542 (2012) 24–27.
[17] S. Berber, Y. Kwon, T. Domanek, Unusually high thermal conductivity of carbon nanotubes, Physical Review Letters 84 (2000) 4613–4616.
[18] P. Kim, L. Shi, A. Majumdar, P.L. McEuen, Thermal transport measurements of individual multiwalled nanotubes, Physical Review Letters 87 (2001) 215502–215505.
[19] B. Munkhbayar, J. Nine, J. Jeoun, M. Bat-Erdene, H. Chung, H. Jeong, Influence of dry and wet ball milling on dispersion characteristics of the multi-walled carbon nanotubes in aqueous solution with and without surfactant, Powder Technology 234 (2013) 132–140.
[20] C.S. Chou, R.Y. Yang, M.H. Weng, C.I. Huang., The applicability of SWCNT on the counter electrode for the dye-sensitized solar cell, Advanced Powder Technology 20 (2009) 310–317.
[21] B. Munkhbayar, J. Nine, Seunghwa Hwang, Junhyo Kim, Kangyoul Bae, Hanshik Chung, Hyomin Jeong. Effect of grinding speed changes on dispersibility of the treated MWCNTs in aqueous solution and its thermal characteristics, Chemical Engineering and Processing 61 (2012) 36–41.
[22] B. Munkhbayar, B. Ochirkhuyag, D. Sarangerel, B. Battsengel, Hanshik Chung, Hyomin Jeong, An experimental study of the planetary ball milling effect on dispersibility and thermal conductivity of MWCNTs – based aqueous nanofluids, Materials Research Bulletin 47 (2012) 4187–4196.
[23] Y. Ding, H. Alias, D. Wen, R.A. Williams, Heat transfer of aqueous suspensions of carbon nanotubes (CNT nanofluids), International Journal of Heat and Mass Transfer 49 (2006) 240–250.
[24] R. Rastogi, R. Kaushal, S.K. Tripathi, A.L. Sharma, I. Kaur, L.M. Bharadwaj, Comparative study of carbon nanotube dispersion using surfactants, Journal of Colloid and Interface Science 328 (2008) 421–428.
[25] S. Huxtable, D.G. Cahill, S. Shenogin, L. Xue, R. Ozisik, P. Barone, Interfacial heat flow in carbon nanotube suspensions, Nature Materials 2 (2003) 731–734.
[26] N. Alexeyeva, J. Kozlova, V. Sammelselg, P. Ritslaid, H. Mändar, K. Tammeveski, Electrochemical and surface characterisation of gold nanoparticle decorated MWCNTs, Applied Surface Science 256 (2010) 3040–3046.
[27] Qingfeng Liu, Wencai Ren, Zhi-Gang Chen, Bilu Liu, Bing Yu, Feng Li, Hongtao Cong, Hui-Ming Cheng, Direct synthesis of carbon nanotubes decorated with size-controllable Fe nanoparticles encapsulated by graphitic layers, Carbon 46 (2008) 1417–1423.
[28] C. Bittencourt, A. Felten, J. Ghijsen, J.J. Pireaux, W. Drube, R. Erni, G. Van Tendeloo, Decorating carbon nanotubes with nickel nanoparticles, Chemical Physics Letters 436 (2007) 368–372.
[29] S.M. Abbasi, A. Nemati, A. Rashidi, K. Arzani, Microstructural features of nanocomposite of Al_2O_3 @CNT/Al_2O_3 nanoparticles synthesized by a solvothermal method, Ceramics International 38 (2012) 3991–3998.
[30] Md.J. Nine, B. Munkhbayar, J.H. Kim, H.S. Chung, H.M. Jeong, Investigation of Al_2O_3-MWCNTs hybrid dispersion in water and their thermal characterization, Journal of Nanoscience and Nanotechnology 12 (2012) 4553–4559.
[31] M. Feng, R.Q. Sun, H.B. Zhan, Y. Chen, Decoration of carbon nanotubes with CdS nanoparticles by polythiophene interlinking for optical limiting enhancement, Carbon 48 (2010) 1177–1185.
[32] Yongbin Zhao, Haijing Liu, Feng Wang, Jingjun Liu, Ki Chul Park, Morinobu Endo, A simple route to synthesize carbon-nanotube/cadmium-sulfide hybrid heterostructures and their optical properties, Journal of Solid State Chemistry 182 (2009) 875–880.
[33] X.L. Luo, A. Morrin, A.J. Killard, M.R. Smyth, Application of nanoparticles in electrochemical sensors and biosensors, Electroanalysis 18 (2006) 319–326.
[34] B. Kim, W.M. Sigmund, Functionalized multiwall carbon nanotube/gold nanoparticle composites, Langmuir 20 (2004) 8239–8242.
[35] V. Georgakilas, V. Tzitzios, D. Gournis, D. Petridis, Attachment of magnetic nanoparticles on carbon nanotubes and their soluble derivatives, Chemistry of Materials 17 (2005) 1613–1617.
[36] P.C. Ma, B.Z. Tang, J.K. Kim, Effect of CNT decoration with silver nanoparticles on electrical conductivity of CNT-polymer composites, Carbon 46 (2008) 1497–1505.
[37] N. Tanakaa, H. Nishikioria, S. Kubotaa, M. Endob, T. Fuji, Photochemical deposition of Ag nanoparticles on multiwalled carbon nanotubes, Carbon 47 (2009) 2752–2754.
[38] P. Garg, J.L. Alvarado, C. Marsh, T.A. Carlson, D.A. Kessler, K. Annamalai, An experimental study on the effect of ultrasonication on viscosity and heat transfer performance of multi-wall carbon nanotube-based aqueous nanofluids, International Journal of Heat and Mass Transfer 52 (2009) 5090–5101.

[39] Y. Zhang, J. Zhao, B. Sun, X. Chen, Q. Li, L. Qiu, F. Yan, Performance enhancement for quasi-solid-state DSSC by using acid-oxidized CNT-based gel electrolyte, Electrochimica Acta. 61 (2012) 185–190.
[40] C. Zhang, L. Ren, X. Wang, T. Liu, Graphene oxide-assisted dispersion of pristine multiwalled carbon nanotubes in aqueous media, Journal of Physical Chemistry C 114 (2010) 11435–11440.
[41] J. Yu, N. Grossiord, C.E. Koning, J. Loos, Controlling the dispersion of MWCNTs in aqueous surfactant solution, Carbon 45 (2007) 618–623.
[42] S. Huh, M. Batmunkh, Y. Kim, H. Chung, H. Jeong, H. Choi, The ball milling with various rotation speeds assisted to dispersion of the MWCNTs, Nanoscience and Nanotechnology Letters 4 (2012) 20–29.
[43] H. Zhong, J.R. Lukes, Interfacial thermal resistance between carbon nanotubes: molecular dynamics simulations and analytical thermal modeling, Physical Review B 74 (2006) 125403–125412.
[44] S.P. Jang, S.U.S. Choi, Role of Brownian motion in the enhanced thermal conductivity of nanofluids, Applied Physics Letters 84 (2004) 4316–4318.
[45] P.M. Ajayan, M. Terrones, A. de la Guardia, V. Huc, N. Grobert, B.Q. Wei, H. Lezec, G. Ramanath, T.W. Ebbesen., Nanotubes in a flash-ignition and reconstruction, Science 296 (2002) 705–718.
[46] H. Xie, L. Chen, Adjustable thermal conductivity in CNT nanofluids, Physics Letters A 373 (2009) 1861–1864.
[47] Y. Xuan, Q. Li, Heat transfer enhancement of nanofluids, International Journal of Heat and Fluid Flow 21 (2000) 58–64.
[48] J.H. Lee, K.Y. Rhee, S.J. Park, Effects of cryomilling on the structures and hydrogen storage characteristics of multi-walled carbon nanotubes, International Journal of Hydrogen Energy 35 (2010) 7850–7857.
[49] A. Nasiri, M.S. Niasar, A.M. Rashidi, R. Khodafarin, Effect of CNT structures on thermal conductivity and stability of nanofluid, International Journal of Heat and Mass Transfer 55 (2012) 1529–1535.
[50] Masami Manabu Ihara, Shiho Inoue. Kanno, Photoabsorption-enhanced DSSC by using localized surface plasmon of silver nanoparticles modified with polymer, Physica E 42 (2010) 2867–2871.
[51] F.P. Incropera, D.P. DeWitt, Fundamentals of Heat and Mass Transfer, 3rd ed., John Wiley & Sons, Inc, Newyork, USA, 1996.
[52] G.W. Lee, J.I. Lee, S.S. Lee, M. Park, J. Kim, Comparisons of thermal properties between inorganic filler and acid-treated multiwall nanotube/polymer composites, Journal of Material Science 40 (2005) 1259–1263.
[53] S. Ghose, K.A. Watson, D.C. Working, J.W. Connell, J.G. Smith, Y.P. Sun, Thermal conductivity of ethylene vinyl acetate copolymer/nanofiller blends, Composites Science and Technology 68 (2008) 1843–1853.